





**Please cite the Published Version**

Whitehead, Kathryn A , Brown, Mark, Caballero, Lucia, Lynch, Stephen , Edge, Michele, Hill, Claire, Verran, Joanna  and Allen, Norman S  (2025) Nano-Titania Photocatalysis and Metal Doping to Deter Fungal Growth on Outdoor and Indoor Paint Surfaces Using UV and Fluorescent Light. *Micro*, 5 (1). 5

**DOI:** <https://doi.org/10.3390/micro5010005>

**Publisher:** MDPI AG

**Version:** Published Version

**Downloaded from:** <https://e-space.mmu.ac.uk/638287/>

**Usage rights:**  [Creative Commons: Attribution 4.0](https://creativecommons.org/licenses/by/4.0/)

**Additional Information:** This is an open access article which first appeared in *Micro*, published by MDPI





**Data Access Statement:** Original/source data for the figures and data in the paper are available from the lead contact upon reasonable request.

**Enquiries:**

If you have questions about this document, contact [openresearch@mmu.ac.uk](mailto:openresearch@mmu.ac.uk). Please include the URL of the record in e-space. If you believe that your, or a third party's rights have been compromised through this document please see our Take Down policy (available from <https://www.mmu.ac.uk/library/using-the-library/policies-and-guidelines>)

## Article

# Nano-Titania Photocatalysis and Metal Doping to Deter Fungal Growth on Outdoor and Indoor Paint Surfaces Using UV and Fluorescent Light

Kathryn A. Whitehead <sup>1,\*</sup>, Mark Brown <sup>2</sup>, Lucia Caballero <sup>1</sup>, Stephen Lynch <sup>3</sup>, Michele Edge <sup>2</sup>, Claire Hill <sup>4</sup>, Joanna Verran <sup>1</sup> and Norman S. Allen <sup>2,\*</sup>

<sup>1</sup> Microbiology at Interfaces, Department of Life Sciences, Faculty of Science and Engineering, Manchester Metropolitan University, Chester Street, Manchester M1 5GD, UK; j.verran@mmu.ac.uk (J.V.)

<sup>2</sup> Division of Chemistry, School of Science and the Environment, Faculty of Science and Engineering, Manchester Metropolitan University, Chester Street, Manchester M1 5GD, UK

<sup>3</sup> Department of Computer Science, Loughborough University, Loughborough LE11 3TU, UK; s.lynch@lboro.ac.uk

<sup>4</sup> Tronox PLC, P.O. Box 26, Grimsby, North-East Lincolnshire DN41 8DP, UK

\* Correspondence: k.a.whitehead@mmu.ac.uk (K.A.W.); norman\_allen@sky.com (N.S.A.)

**Abstract:** This work determined the resistance of paint formulations containing TiO<sub>2</sub> particles to fungal growth. Siloxane, acrylic and silicone paints were placed outdoors, and the fungal species growing thereon were recorded after 3, 6 and 9 months. In addition, three paint types containing TiO<sub>2</sub> with/without biocide were inoculated with fungal spores and irradiated using UV. Acrylic paints were also doped with different metals and were inoculated and incubated under fluorescent light. Following outdoor incubation, the silicone paint was the least colonised by different fungal species. The species most recovered from the surfaces were *Aspergillus* spp. and *Penicillium* spp. Following UV irradiation on different paints containing biocide and/or a photocatalyst, no fungal growth was demonstrated on some of the paint combinations. When the paint samples were doped with different metals and incubated using light, the sample most efficient at preventing fungal growth contained lanthanum (0.004%). The paint samples containing praseodymium (light:1.72) facilitated the densest fungal colonies. Most of the surfaces demonstrated heterogeneous coverage by the fungi. The most clustered fungal colonisation was on surfaces incubated in the light. This work demonstrated that fungal colonisation on paints changed over time and that the antimicrobial efficacy of TiO<sub>2</sub> was affected by the chemical composition, biocide and doping of the paint.

**Keywords:** titanium dioxide; photocatalyst; fungi; *Aspergillus*; paint; multifractal analysis



Academic Editor: Eva Kowalska

Received: 14 November 2024

Revised: 10 January 2025

Accepted: 21 January 2025

Published: 28 January 2025

**Citation:** Whitehead, K.A.; Brown, M.; Caballero, L.; Lynch, S.; Edge, M.; Hill, C.; Verran, J.; Allen, N.S.

Nano-Titania Photocatalysis and Metal Doping to Deter Fungal Growth on Outdoor and Indoor Paint Surfaces Using UV and Fluorescent Light.

*Micro* **2025**, *5*, 5. <https://doi.org/10.3390/micro5010005>

**Copyright:** © 2025 by the authors. Licensee MDPI, Basel, Switzerland. This article is an open access article distributed under the terms and conditions of the Creative Commons Attribution (CC BY) license (<https://creativecommons.org/licenses/by/4.0/>).

## 1. Introduction

Biological corrosion or biodeterioration is a complex process that involves the destruction of materials by living organisms which include fungi, and these phenomena are problematic in both old and new buildings [1]. The most common culturable airborne fungi, both indoors and outdoors and in all seasons and regions, have been demonstrated to be *Cladosporium*, *Penicillium*, nonsporulating fungi and *Aspergillus* [2]. The most versatile fungal strains involved in polymer degradation are *Aspergillus*, *Penicillium* and *Aureobasidium* spp. [3]. Among the most harmful pathogens to humans are fungi of the genera *Alternaria*, *Aspergillus*, *Cladosporium*, *Penicillium*, *Fusarium*, *Rhizopus* and *Stachybotrys* [1]. Exposure to fungi has been reported to cause several types of human health problems,

primarily irritations, infections, allergies and toxic effects, and it has been suggested that toxigenic fungi can be the cause of additional adverse health effects [2].

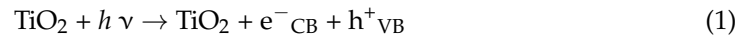
In recent decades, there has been a great deal of commercial interest and extensive development of light-stable surface coatings with the ability to actively catalyse the degradation of harmful organic pollutants into environmentally acceptable waste products. Self-disinfecting thin films have become particularly attractive in places such as hospitals and care facilities to reduce the spread of infections, as well as in public facilities such as commercial centres, schools, kitchens, baths and floors [4]. Therefore, for example, an important application of TiO<sub>2</sub> in the nanoparticle size is the disinfection of surfaces by photocatalytic oxidation [5,6].

Titanium dioxide is a white pigment used in the paint industry. Generally, TiO<sub>2</sub> is an n-type wide band gap semiconductor material which the absorption of light can chemically activate. Conventional TiO<sub>2</sub> pigments comprise discrete particles of a mean crystallite size of around 0.2–0.3 μm. Particles of this size reflect all the wavelengths of visible light, producing the effect of whiteness on the human eye. Over the last five decades, new applications of TiO<sub>2</sub> as a photocatalyst have appeared; the aim is to use the TiO<sub>2</sub> photocatalyst in a surface matrix, which, when irradiated with light, will decompose dirt and microorganisms [7–11]. This is more commonly now referred to as Nano-TiO<sub>2</sub>.

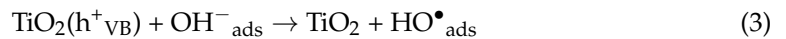
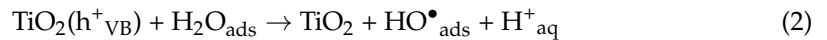
During the photocatalytic process, the illumination of a TiO<sub>2</sub> semiconductor with UV generates an electron–hole pair that takes part in creating a subsequent redox environment at the surface of the TiO<sub>2</sub> [1]. Two crystalline forms of TiO<sub>2</sub> have photocatalytic activity, anatase and rutile, with the former being more active. The TiO<sub>2</sub> photocatalytic process involves several chemical steps that produce reactive species, which, in principle, can cause fatal damage to a microbial cell. After absorption of radiation equivalent to the band gap energy of the semiconductor ( $\lambda < 388$  nm for anatase), electrons (e) are excited from the valence band to the conduction band of the semiconductor and holes are left in the valence band. These electron (e)/hole (h<sup>+</sup>) pairs that form within the particle can undergo subsequent oxidation and reduction reactions with any species that might be adsorbed on the surface of the semiconductor, and h<sup>+</sup> and e<sup>−</sup> are powerful oxidising and reducing agents, respectively. Excited-state conduction band electrons and valence band holes can recombine and dissipate the input energy as heat, or they can react with electron donors and acceptors that are adsorbed on the semiconductor surface, depending on the reaction conditions and molecular structures of the semiconductor [12]. In the presence of the appropriate redox couples, these charge carriers induce reduction reactions and oxidation. The strong oxidation power of photogenerated holes on the catalyst's surface enables it to react with physisorbed water or chemisorbed OH<sup>−</sup> at the catalyst/water interface. This produces highly reactive hydroxyl radicals (•OH) that are also powerful oxidants. In the conduction band, the reducing power of the electrons can induce the reduction of molecular oxygen (O<sub>2</sub>) to form the superoxide ion (O<sub>2</sub>•<sup>−</sup>). This reaction prevents e<sup>−</sup>/h<sup>+</sup> recombination in the absence of other electron acceptors [13]. The superoxide ion and its protonated form subsequently dismutate to form stable products. The effects of photocatalytic degradations can result from H<sub>2</sub>O<sub>2</sub> being present, which may enhance or decrease photocatalytic degradation [14].

The chemical steps in the photocatalytic process occur after the absorption of radiation equivalent to the band gap energy of the semiconductor ( $\lambda < 388$  nm for anatase). Then, electrons (e<sup>−</sup>) are excited from the valence band (VB) to the conduction band (CB) of the semiconductor, and holes are left in the valence band. These electron (e<sup>−</sup>)/hole (h<sup>+</sup>) pairs, formed within the particle [Reaction (1)], can undergo subsequent oxidation and reduction

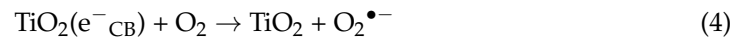
reactions with any species that might be adsorbed on the surface of the semiconductor. In this reaction,  $h^+$  and  $e^-$  are powerful oxidising and reducing agents, respectively.



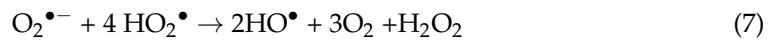
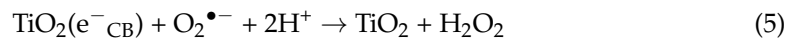
In the presence of the appropriate redox couples, these charge carriers are able to induce reactions and oxidations, and the strong oxidation power of the photogenerated holes (Reaction (1)) on the catalyst surface enables it to react with physisorbed water or chemisorbed  $\text{OH}^-$  at the catalyst/water interface. This produces highly reactive hydroxyl radicals ( $\bullet\text{OH}$ ) that are also powerful oxidants (Reactions (2) and (3)).



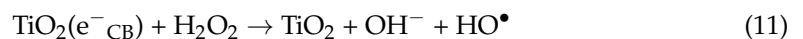
In the conduction band, the reducing power of the electrons can induce the reduction of molecular oxygen ( $\text{O}_2$ ) to form the superoxide ion ( $\text{O}_2^{\bullet-}$ ) (Reaction (4)). This reaction prevents  $e^-/h^+$  recombination in the absence of other electron acceptors [13].



The superoxide ion and its protonated form subsequently dismute to form stable products (Reactions (5)–(9)) [15]:

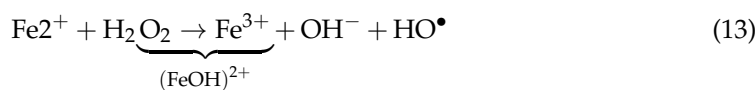


The presence of  $\text{H}_2\text{O}_2$  can increase photodegradation due to the production of  $\text{HO}^{\bullet}$  radicals (Reaction (10)) or the reduction of  $\text{H}_2\text{O}_2$  (Reaction (11)) [14]. In addition, irradiated  $\text{TiO}_2$  can be degraded over the band gap (Reaction (12)).



Upon absorption of the UV spectrum of light, photocatalysis has been found to decompose organic materials and inactivate bacteria, algae, filamentous and unicellular fungi, mammalian viruses, bacteriophage, protozoa and viruses [7–10]. The reactive oxygen species that are generated may disrupt or damage the cells or structures adsorbed on the  $\text{TiO}_2$  surface, resulting in the death of the microorganisms. Among all the active species generated, the hydroxyl radicals are thought to be the most important oxidant species responsible for microbial inactivation [15]. There is evidence that the  $\bullet\text{OH}$  that is generated by hole transference does not diffuse from the surface of the  $\text{TiO}_2$  into the bulk aqueous phase; thus, the inactivation of *Escherichia coli* (a bacterium) by hydroxyl radicals that are generated by photocatalytic action is dependent on the mass transfer limitations through the cell wall or cell membrane and the short half-life of the radical. Hydrogen peroxide

can enter the cell and be activated by ferrous ions via the Fenton reaction, thus possibly contributing to the acceleration of bacterial inactivation (Reactions (13) and (14)) [11,15].



Therefore, while the  $\text{TiO}_2$  is being illuminated and the membrane perforated by the reactive oxygen species, ferrous ( $\text{Fe}^{2+}$ ) and ferric ions ( $\text{Fe}^{3+}$ ) could be released. The positive effect of irradiation on the deterioration of the cell is due to the chemical regeneration of ferrous ions by photoreduction of aqua complexes of ferric ions, which leads to additional  $\text{OH}^\bullet$  being formed (Reaction (14)). The Fenton reaction may take place in vivo, producing more damaging hydroxyl radicals [13]. The newly generated  $\text{Fe}^{2+}$  reacts with  $\text{H}_2\text{O}_2$ , generating a second  $\text{OH}^\bullet$  and ferric ion (Reaction (13)), and the cycle continues [15].

Most surfaces are tested using UV, and one drawback of  $\text{TiO}_2$  is its wide band gap, as it does not absorb light in the visible region of the spectrum. Only 5–8% of sunlight is composed of UV light, and with the photonic efficiency of  $\text{TiO}_2$  being less than 10%, it is important to find ways in which to reduce the band gap energy to enable visible absorption, thus enhancing photocatalytic efficiency. Metal ion doping reduces the band gap and also shifts the absorption into the visible spectrum. In addition,  $\text{TiO}_2$  is a semiconductor whose photocatalytic properties deteriorate under visible light due to its wide band gap. The doping of  $\text{TiO}_2$  with various elements increases its photocatalytic activity due to the formation of new energy levels near the conduction band, and it is known that doping increases the photocatalytic activity of  $\text{TiO}_2$  upon irradiation with visible light. Hence, testing samples in real-world environments under fluorescent lights provides further information on the antimicrobial efficacy of  $\text{TiO}_2$ , which is relevant when increasing the technology readiness level of the product.

This work aimed to identify the key fungal species that colonised paint surfaces over time when exposed to the outdoor environment for nine months. Using a selected key coloniser species, paint samples were also tested using UV to determine the efficacy of fungal kill on paints containing  $\text{TiO}_2$  with and without commercial biocide. Finally,  $\text{TiO}_2$  paints doped with metal ions were irradiated with fluorescent light to determine the efficacy of the paints as a deterrent to fungal colonisation.

## 2. Methods

### 2.1. Paint Preparation

The water-based acrylic formulation (Rohm and Haas, Bensalem, PA, USA) was based on two components, part A and part B. Part A consisted of water (75 g), Primal AC-337 (61.3 g), Texanol (2.3 g), BYK-ammonia (0.3 g) and 024 (0.1 g). Part B was composed of water (95 g), Acrysol RM-12W (12 g) and Acrysol 2020 (3.5 g). Part A and part B were mixed, B and the additives were added, and then the suspension was stirred for 10 min. Part B (50% *w/w*) was added and mixed for 5 min. The silicate paint used in this study was a standard commercial (Wacker Chemie, Munich, Germany) AG SILRES BS45 water-based emulsion. The siloxane paint was a standard paint obtained from Tronox, UK. The nanotitania particles (Ultrafine and Speciality Titanium dioxide: CristalACTiV™ Anatase PC-500 surface area 300 m<sup>2</sup>/g) were dispersed throughout the paints using a high-speed laboratory mixer (2000 rpm) to remove any conglomeration. In cases where the formulations did not work, they were not tested with fungal species. The control paints comprised the base paint with no added titania or biocides.

## 2.2. Determination of Fungal Species Following 9 Months of Outdoor Exposure

Three replicates of each paint (siloxane, acrylic and silicone) in standard dispersions were drawn down onto 5 cm × 10 cm aluminium substrates using a K bar, dried overnight and fixed to a stainless-steel frame. The paint samples were placed at angles of 45° outdoors in Manchester, UK, from March to December, where the temperatures ranged from 3 °C to 25 °C. The 45° angle was determined to allow water runoff but also so that the surfaces were not shielded from the environment. The fungal colonisation on the paints was tested at 3, 6 and 9 months by removing the plates and using direct contact by pressing the paint sample for 10 s onto a Sabouraud agar plate (Oxoid, Basingstoke, UK) or by swabbing the paint 10 times from top to bottom, then left to right, and transferring it to a Sabouraud agar plate. The plates were incubated for up to 1 month at 25 °C until good growth of all species potentially present had occurred. The fungal samples were identified by subculturing the fungal isolates onto Sabouraud agar and potato dextrose agar (Oxoid, UK). These samples were again incubated for up to 1 month at 25 °C until good growth had formed. Any pigmentation of the fungal growth on the agar was noted. Drop slides were produced by pacing a 100 µL drop of molten agar onto a glass slide that had been previously sterilised with 70% ethanol (BDH, Bury, UK). The agar was set for 30 min in a class 2 cabinet. The agar drop was cut in half using a sterile scalpel, and a small sample of the purified fungal culture was removed from the agar plate using the scalpel and placed in between the segmented agar droplets. The inoculated glass slide was placed inside a sterile Petri dish and incubated at 25 °C until observable growth had formed (up to seven days or until good growth had formed). The fungal growth was examined using light microscopy (Nikon, Surrey, UK) and imaged using Cell F software v1 17. The fungi were identified using a method based on pigmentation and hyphal and conidial shape and size.

### 2.2.1. Preparation of *A. niger* Spores

The preparation of the *A. niger* spores was carried out in accordance with the standard test method for determining the resistance of paint films and related coatings to fungal defacement using the accelerated four-week agar plate assay [16] by taking an inoculum from a fungal slope in long-term storage and streaking it onto potato dextrose agar (Oxoid, UK) using a swab that had been pre-wetted in Sabouraud broth (Oxoid, UK). This was incubated at 30 °C for 5 days. Sabouraud broth (5 mL) was pipetted onto the culture using a sterile glass Pasteur pipette, which was rubbed across the surface up and down and side to side to free the conidia from the fungal mat. The resultant fungal spore suspension was collected and stirred for 30 min, then filtered using glass wool (VWR, Dorset, UK) under sterile conditions. The spores were harvested using centrifugation (1721 rpm for 10 min), then washed in sterile distilled water 3 times and finally re-suspended to an optical density of  $1.0 \pm 0.1$  (610 nm). This equated to  $1.0 \pm 0.45 \times 10^6$  spores cm<sup>2</sup>, and these were stored at 4 °C until use for up to 1 month. The spore count was determined using a haemocytometer (Thermo Fisher Scientific, Warrington, UK) [17–19].

### 2.2.2. Exposure of Different Paint Formulations Containing Commercial Biocide, TiO<sub>2</sub> (Nano-Titania) or Commercial Biocide and TiO<sub>2</sub> Seeded with *A. niger* Spores

Different paint formulations (siloxane, acrylic, silicate) were produced containing commercial biocide (Cavasol Cyclodextrin biocide formulated by Wacker Chemie AG), TiO<sub>2</sub> (Nano-Titania PC-500 Tronox PLC, Stallingborough, UK) or commercial biocide. The paints were drawn down using a K bar onto a 30 mm × 30 mm polymer film and placed facing paint-side upwards onto Sabouraud agar. One hundred microliters of *A. niger* spore suspension was placed onto the surface and spread using a sterile spreader across the paint surface, taking care not to spill it onto the agar. The paint samples were incubated at

25 °C. Two replicate sets were placed into the incubator, and on each day of the experiment, one was removed and irradiated daily for 10 min. The second set remained in the dark (control) ( $n = 3$ ). A high-pressure mercury lamp, which emits primarily in the blue-green wavelengths UV-A (around 400 nm), UVB (280–315 nm) or UV-C (around 250 nm) was used to irradiate the samples, providing a light intensity in the region of 27 W/m<sup>2</sup>. Binary images were obtained from the original images, and the percentage coverage was computed for the irradiated and doped surfaces.

### 2.2.3. Effect of Chemical Doping on *A. niger* Growth on the Paint Surfaces

Acrylic resin (Tronox, Grimsby, UK) was used as the paint base formulation with nano-titania. The nano-titania was mixed with no metals (control) or praseodymium, lanthanum, manganese, iron, chromium, niobium, lithium, tungsten, molybdenum or neodymium (Tronox, Grimsby, UK). Then, they were fired for 1 h at 400 °C to retain the crystal phase of the anatase and to maintain the high surface area. The nano-titania with/without dopant was then added to the acrylic paint at 0.25%  $w/v$ .

The samples were cut into 30 mm × 30 mm pieces, and 100 µL of the prepared *A. niger* spore suspension was added to the surfaces ( $n = 3$ ). The inoculated samples were incubated at 20 °C for four weeks under fluorescent lamps (Silvania Italia, Winnipeg, Canada), which were fitted in an Illuminated Cooled Incubator (Gallenkamp, Cambridge, UK), which had an energy output of 8 W and a wavelength of 300–700 nm and were 150 mm from the samples. Pictures were taken of the samples after 4 weeks of incubation. Binary images were obtained from the original images, and the percentage coverage was computed for the irradiated and doped surfaces. A multifractal analysis was applied to measure the density, dispersion and clustering of the binary images.

### 2.2.4. Multifractal Analysis

Using packages such as Python v3 [20] and MATLAB® vR2024b [21], binary images were obtained, and a multifractal analysis was applied to measure the density, dispersion and clustering of fungal growth on different paint surfaces. The  $q$ 'th moment (or partition function)  $Z_q$  was defined by:

$$Z_q = \sum_{i=1}^n p_i^q(\ell),$$

where  $p_i$  were the weights (or probabilities) that sum to one,  $\ell$  was the length scale, and  $q$  was a parameter. A scaling function labelled  $\tau(q)$  satisfied the equation:

$$\sum_{i=1}^n p_i^q r_i^{\tau(q)} = 1,$$

with  $r_i$  fragmentation ratios, and this was defined by:

$$\tau(q) = \frac{\log_e(Z_q(\ell))}{-\log_e(\ell)},$$

where  $\log_e$  was the natural logarithm. The multifractal  $f(\alpha)$  curve can be plotted using the parametric equations:

$$f(\alpha) = q\alpha(q) + \tau(q) \text{ and } \alpha = -\frac{d\tau}{dq}.$$

To illustrate the analysis, consider the binary images given for two examples. The  $f(\alpha)$  curve gives the following information, as demonstrated in the binary images displayed in Figures 1 and 2.

The fractal dimension density  $D_0$ , ( $D_0 = f(\alpha_0)$ ), is a measure of how densely the material covers the surface. In Figure 1A, the image gives rise to a  $f(\alpha)$  curve and a

dispersion across the surface where  $D_0 = 1.239$ , whereas for Figure 2A, the corresponding  $f(\alpha)$  curve gives a  $D_0 = 1.849$ .

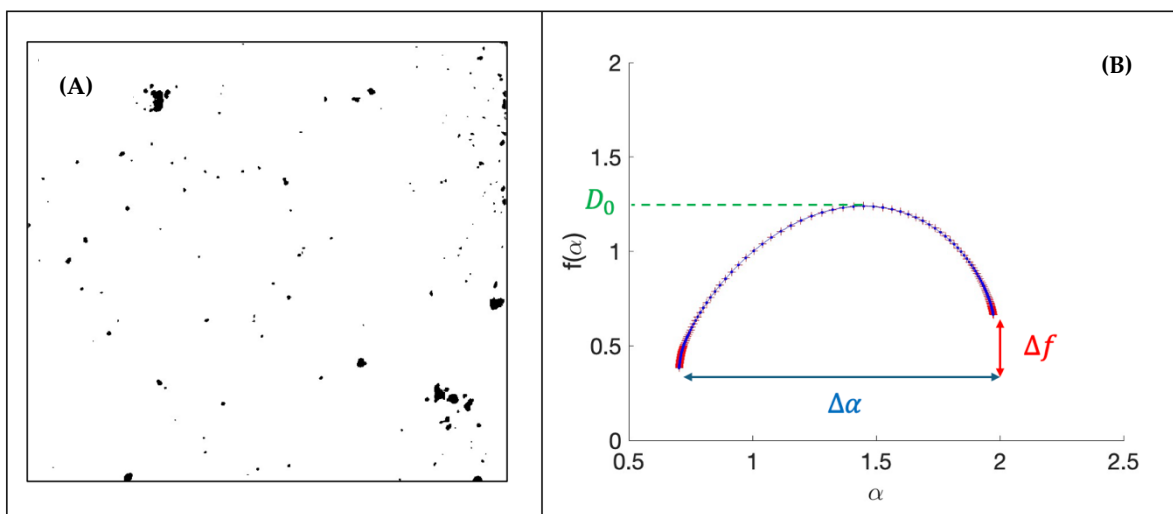


**Figure 1.** (A) Binary image of fungal growth on a surface. (B) Multifractal  $f(\alpha)$  curve. The density is low, the dispersion is high, and the clustering is negative, representing a lack of clustering of dark matter on a white background. Readers should note that identical  $f(\alpha)$  curves are plotted if the white and black pixels are interchanged in the binary images.

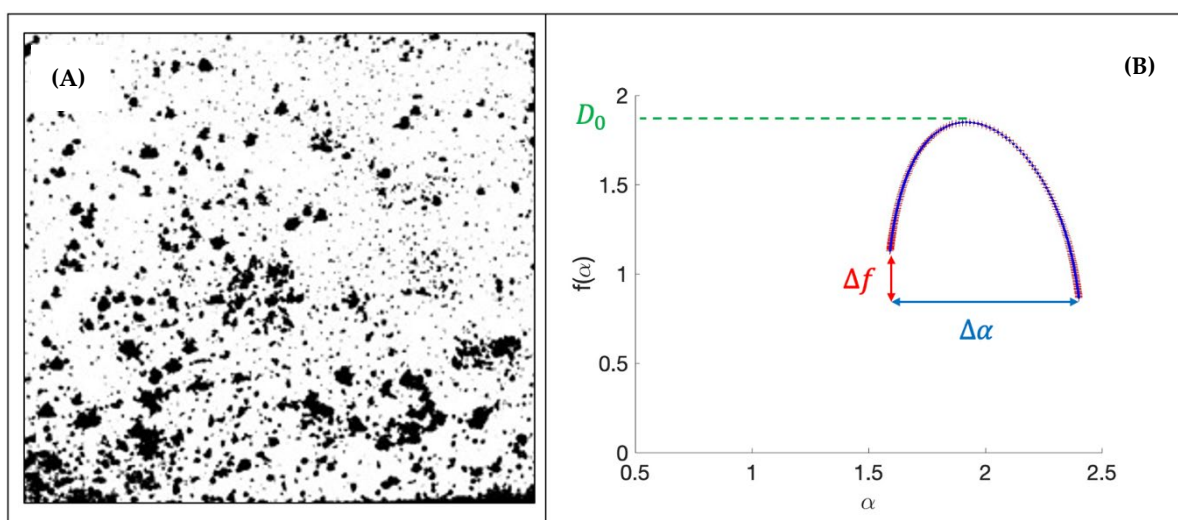


**Figure 2.** (A) Binary image of fungal growth on a surface. (B) Multifractal  $f(\alpha)$  curve. The density is high, the dispersion is low, and the clustering is positive, representing the clustering of dark matter on a white background.

The width of the  $f(\alpha)$  curve gives the value of the dispersion across a surface, and the dispersion is given by the blue double-headed line.

$$\Delta\alpha = \alpha_{max} - \alpha_{min},$$

The dispersion ( $\Delta\alpha$ ) is how evenly or unevenly the points are dispersed over the surface. In Figure 1,  $\Delta\alpha = 1.256$ , whereas in Figure 2, the corresponding  $f(\alpha)$  curve gives a density of  $\Delta\alpha = 0.809$ .

The asymmetry in the  $f(\alpha)$  curves give a measure of clustering, where

$$\Delta f(\alpha) = f(\alpha_{min}) - f(\alpha_{max}),$$



and this is depicted by the red double-arrow line. In Figure 1,  $\Delta f(\alpha) = -0.314$ , and for Figure 2B, the corresponding  $f(\alpha)$  curve gives a clustering value of  $\Delta f(\alpha) = 0.263$ .

### 3. Results

Comparisons were made of a range of paint formulations to withstand fungal colonisation; in the outdoor environment, following irradiation with UV on paints containing photocatalysts and/or biocides and on paints doped with a range of metals irradiated using fluorescent light.

#### 3.1. Growth and Identification of Fungal Species Following 9 Months of Outdoor Exposure

The outdoor paint trial on the acrylic paint took place over 9 months to determine the number and changes in the colonisation of the fungal species on the paints over time. Following removal of the paints from the outdoor environment, the fungal species were recovered after 3 months (Figure 3A) and 9 months (Figure 3B). Following the recovery of the fungal species, the fungi were isolated so that their genus could be determined using traditional microbiological techniques. The most prevalent genera were *Penicillium* spp. (Figure 3C,E) or *Aspergillus* spp. (Figure 3D).

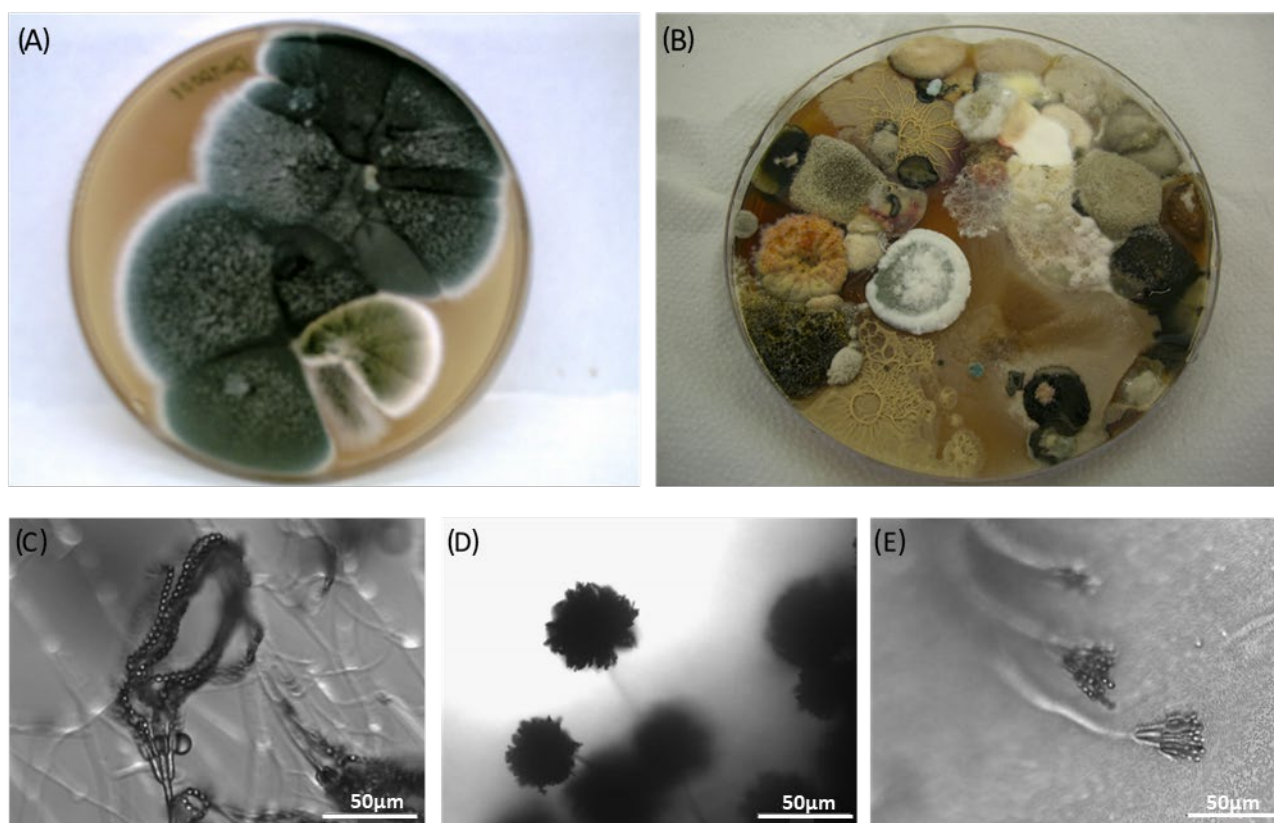


**Figure 3.** Fungal growth on contact plates following recovery of the paint samples from outdoors after (A) 3 months and (B) 9 months. Identification of fungal species following isolation and drop slide preparation: (C) *Penicillium* spp., (D) *Aspergillus niger* and (E) *Penicillium* spp.

The number of different fungal species was assessed following recovery from the outdoor paint samples (Table 1). Following 3 months of outdoor exposure, the number of different fungal species recovered varied between 14 (siloxane), 16 (acrylic) and 10 (silicone) (Table 1A) compared to the control, with seven species recovered. However, following 6 months of outdoor exposure, the number of different fungal species recovered had decreased on all the surfaces (12 siloxane and acrylic, eight silicones and four control)

(Table 1B), with the exception of the acrylic surface, on which the numbers of fungal species recovered remained the same as for the 6-month period (12 on acrylic surfaces). The number of fungal species increased again on the different paints (13 siloxane, 11 silicone and 10 control) (Table 1C). Overall, fewer fungal species were recovered from the silicone paint at all time points.

**Table 1.** Fungal species recovered from the outdoor paint formulations following (A) 3 months, (B) 6 months and (C) 9 months of outdoor exposure. Pen = *Penicillium* spp., Asp = *Aspergillus* spp., Gli = *Gliocladium* spp., Y = Yeast, Hun = *Humicola* spp., Pae = *Paecilomyces* spp., Gli = *Gliocladium* spp. and Cla= *Cladsporium* spp. Grey boxes indicate recovered species, and white boxes indicate that the fungal species was not recovered.

| Type of Paint | Fungal Species Recovered |       |       |       |       |       |       |       |       |       |       |       |       |       |       | Total |
|---------------|--------------------------|-------|-------|-------|-------|-------|-------|-------|-------|-------|-------|-------|-------|-------|-------|-------|
| (A)           | Pen1                     | Asp1  | Gli   | Asp2  | Asp3  | Asp4  | Pen2  | Asp5  | Asp6  | Y1    | Hun   | Pae   | Y2    | Gli   | Cl    | Total |
| Siloxane      | Grey                     | Grey  | Grey  | Grey  | Grey  | Grey  | Grey  | Grey  | Grey  | Grey  | White | Grey  | Grey  | Grey  | White | 14    |
| Acrylic       | Grey                     | Grey  | White | Grey  | Grey  | Grey  | Grey  | Grey  | Grey  | Grey  | White | Grey  | Grey  | Grey  | White | 16    |
| Silicone      | Grey                     | White | White | White | White | White | White | White | White | White | White | White | White | White | White | 10    |
| Control       | White                    | White | White | White | White | White | White | White | White | White | White | White | White | White | White | 7     |
| (B)           | Pen1                     | Asp1  | Gli   | Asp2  | Asp3  | Asp4  | Pen2  | Asp5  | Asp6  | Y1    | Hun   | Pae   | Y2    | Gli   | Cl    | Total |
| Siloxane      | Grey                     | Grey  | Grey  | Grey  | Grey  | Grey  | Grey  | Grey  | Grey  | Grey  | White | Grey  | Grey  | Grey  | White | 12    |
| Acrylic       | Grey                     | Grey  | White | Grey  | Grey  | Grey  | Grey  | Grey  | Grey  | Grey  | White | Grey  | Grey  | Grey  | White | 12    |
| Silicone      | Grey                     | White | White | White | White | White | White | White | White | White | White | White | White | White | White | 8     |
| Control       | White                    | White | White | White | White | White | White | White | White | White | White | White | White | White | White | 4     |
| (C)           | Pen1                     | Asp1  | Gli   | Asp2  | Asp3  | Asp4  | Pen2  | Asp5  | Asp6  | Y1    | Hun   | Pae   | Y2    | Gli   | Cl    | Total |
| Siloxane      | Grey                     | Grey  | Grey  | Grey  | Grey  | Grey  | Grey  | Grey  | Grey  | Grey  | White | Grey  | Grey  | Grey  | White | 13    |
| Acrylic       | Grey                     | Grey  | White | Grey  | Grey  | Grey  | Grey  | Grey  | Grey  | Grey  | White | Grey  | Grey  | Grey  | White | 12    |
| Silicone      | Grey                     | White | White | White | White | White | White | White | White | White | White | White | White | White | White | 11    |
| Control       | White                    | White | White | White | White | White | White | White | White | White | White | White | White | White | White | 10    |

The fungi were identified to the genus level following their recovery from the outdoor paint samples (Table 1). The fungal species that were recovered from each paint were different at different time points. At month 3, all the fungal species were recovered from the siloxane paint apart from the *Humicola* spp. and *Cladsporium* spp., whilst, on the acrylic paint, only the *Cladsporium* spp. was not recovered. The silicone did not demonstrate the recovery of *Aspergillus* 2 or 5 spp., *Penicillium* spp. 2, *Paecilomyces* spp. or *Cladsporium* spp. The control paint demonstrated the least number of fungal species and did not recover the growth of *Aspergillus* spp. 1, 2 or 6, *Penicillium* 2 spp., *Humicola* spp., *Paecilomyces* spp., yeast 2 or *Cladsporium* spp.

Following 6 months of environmental exposure, on the siloxane paint, *Penicillium* 2 spp., *Aspergillus* 6 spp. and the *Humicola* spp. were not recovered, whilst on the acrylic paint, *Aspergillus* 2 spp., *Humicola* spp., *Gliocladium* spp. and the *Cladsporium* spp. were not recovered. On the silicone paint, *Aspergillus* 3, 5 and 6 spp., *Penicillium* 2 spp., *Humicola* spp., *Paecilomyces* spp. and *Cladsporium* spp. were not recovered. On the control surface, only four fungal species were recovered: *Gliocladium* spp., *Aspergillus* 2 spp., yeast 1 and *Humicola* spp.

After 9 months of outdoor exposure, yeast 2 and *Cladsporium* spp. did not grow on any of the paints or control surfaces. On the siloxane paint, *Penicillium* 2 spp. was also not recovered, whilst on the acrylic paint, *Aspergillus* 6 sp. and *Humnicola* spp. were not recovered. On the silicone paint, *Gliocladium* spp. and *Aspergillus* 3 and 6 spp. were not recovered, whilst on the control paint surface, *Penicillium* 1 and 2 spp., *Gliocladium* spp. and *Aspergillus* 6 spp. were not recovered. The most recovered species from the surfaces were *Aspergillus* spp. and *Penicillium* spp.

### 3.2. Exposure of Different Paint Formulations Seeded with *A. niger* Spores and Exposed to UV

Different paint formulations were used to determine how the growth of fungi was reduced using UV compared to the reduction of fungal growth under dark conditions (Figure 4). The different paint formulations (siloxane, acrylic and silicate) were prepared containing commercial biocide,  $\text{TiO}_2$  or commercial biocide and  $\text{TiO}_2$ . The paint formulations were seeded with fungal spores, and the growth was determined using multifractal analysis. The results demonstrated that a number of surfaces showed no growth (siloxane with a photocatalyst in the dark, siloxane with a photocatalyst and biocide in the light, acrylic in the light or dark, acrylic with a photocatalyst and biocide in the dark, and silicate in the dark). Low fungal growth was demonstrated on the siloxane in light (0.004) or dark conditions (0.005), siloxane with a photocatalyst and biocide in the dark (0.004), acrylic with a photocatalyst in the light (0.003) or dark (0.001), or silicate in the light (0.003). Paint samples that demonstrated a high degree of fungal growth included siloxane with biocide in the light (0.15) or dark (0.09), acrylic with biocide in the light (0.08), or acrylic with a photocatalyst and biocide in the light (0.04).

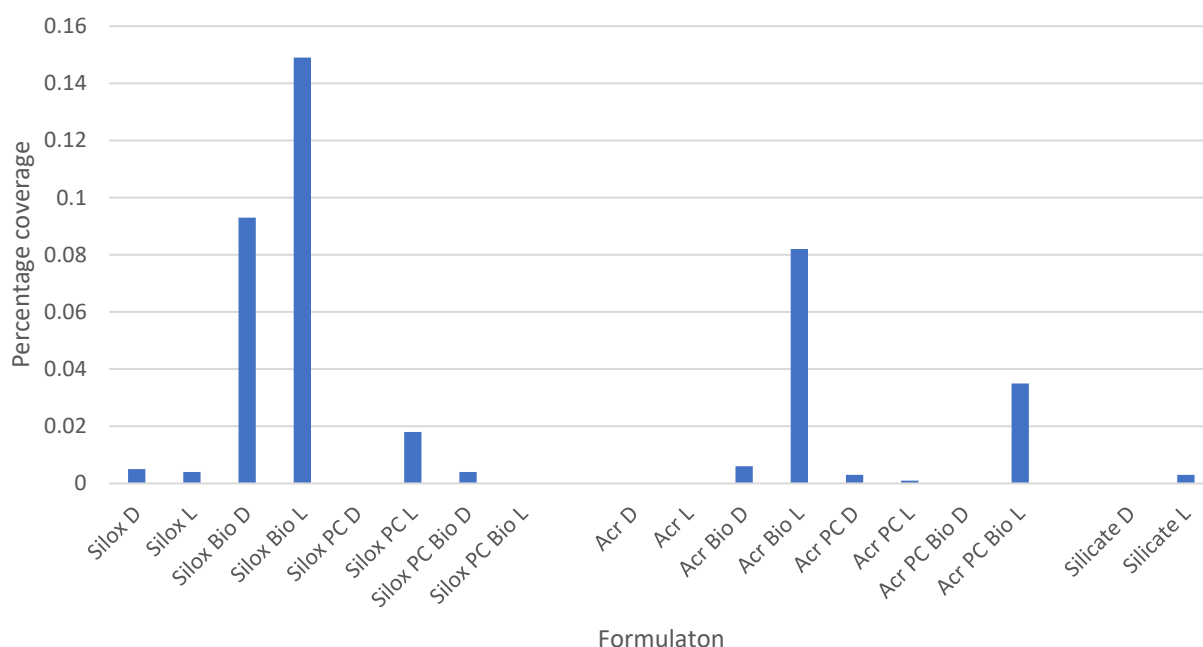


**Figure 4.** Coverage of fungi on paint surfaces with commercial biocide,  $\text{TiO}_2$  or  $\text{TiO}_2$  and commercial biocide. Results following UV irradiation or in dark conditions. Silox = siloxane paint, Acr = acrylic paint, L = light conditions, D = dark conditions, PC = addition of photocatalyst and Bio = addition of biocide.

### 3.3. Effect of Chemical Doping on *A. niger* Growth on the Paint Surfaces Under Fluorescent Lights

When the paint samples were doped with different elements and incubated under fluorescent lights or kept in the dark (Figure 5), the doped surfaces that developed the least fungal growth in the light were manganese (0.03%), molybdenum (0.03%) and lanthanum (0.04%), whilst in the dark, they were molybdenum (0.01%), iron (0.03%), lanthanum (0.04%) and tungsten (0.07%).

The samples that resulted in the most fungal growth in the light were those surfaces doped with chromium (0.99%), tungsten (0.91%) and lithium (0.64%), and in the dark, lithium (0.3%), neodymium (0.14%) and manganese (0.13%). It was also demonstrated that some of the samples grown in the dark generally demonstrated less fungal growth than those grown under the light conditions.

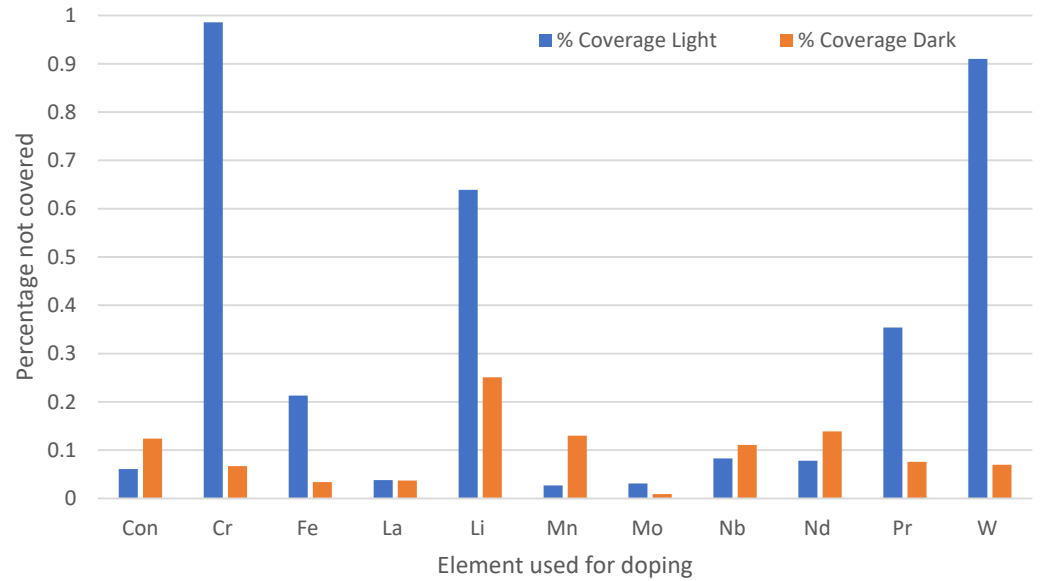


**Figure 5.** Percentage of no fungal growth on paint surfaces doped with 0.25% of the elements: Con = control, Cr = chromium, Fe = iron, La = lanthanum, Li = lithium, Mn = manganese, Mo = molybdenum, Nb = niobium, Nd = neodymium, Pr = praseodymium and W = tungsten.

The results of the density of the fungi across the surfaces demonstrated that paints doped with praseodymium (1.72), tungsten (1.62) and molybdenum (1.37) incubated in the light produced more dense fungal colonies than those incubated in the dark (Figure 6). The surfaces incubated under dark conditions demonstrated more dense fungal colonies for most of the doped paints, with the greatest differences observed for those surfaces doped with chromium (1.20 light:1.65 dark), lithium (1.54 light:1.85 dark) and manganese (1.43 light:1.69 dark).

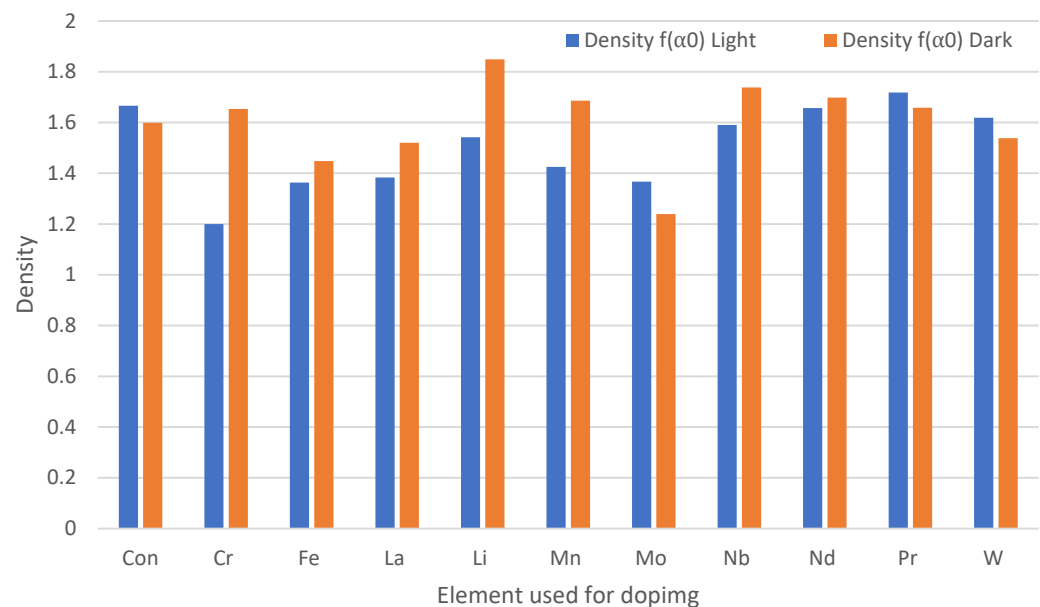


**Figure 6.** Density of fungal growth on paint surfaces doped with 0.25% of the elements Con = control, Cr = chromium, Fe = iron, La = lanthanum, Li = lithium, Mn = manganese Mo = molybdenum, Nb = niobium, Nd = neodymium Pr = praseodymium and W = tungsten.

Following incubation of the doped paint surfaces, the surfaces that demonstrated more heterogeneous dispersions of fungi across the surfaces included those that contained the metals iron (dark: 1.32), lithium (dark: 1.31), manganese (Light: 1.26), molybdenum

(dark: 1.26) and iron (light: 1.25) (Figure 7). Most of the surfaces demonstrated heterogeneous surface coverage by the fungi. The most homogeneous dispersion of the fungi across the surfaces was with praseodymium (light: 0.48), whilst with lithium (light: 0.5), growth was dispersed across the surface in a symmetrical fashion.

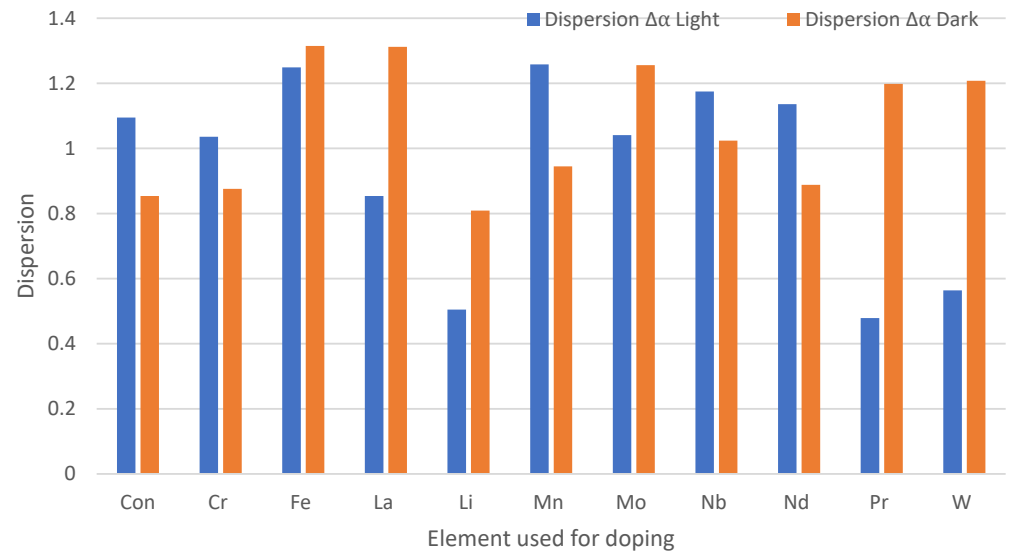


**Figure 7.** Dispersion of fungal growth on paint surfaces doped with 0.25% of the elements: Con = control, Cr = chromium, Fe = iron, La = lanthanum, Li = lithium, Mn = manganese, Mo = molybdenum, Nb = niobium, Nd = neodymium, Pr = praseodymium and W = tungsten.

Tungsten (light: 0.64), praseodymium (light: 0.51), lithium (light: 0.48) and chromium (light: 0.38) demonstrated the most clustering of the fungal species on the surfaces, whilst iron (dark:  $-0.56$ ), lanthanum (dark:  $-0.52$ ) and tungsten (dark:  $-0.46$ ) demonstrated the least clustering of the fungi across the surfaces (Figure 8). Overall, surfaces incubated in the dark demonstrated less clustering than those incubated in the light.

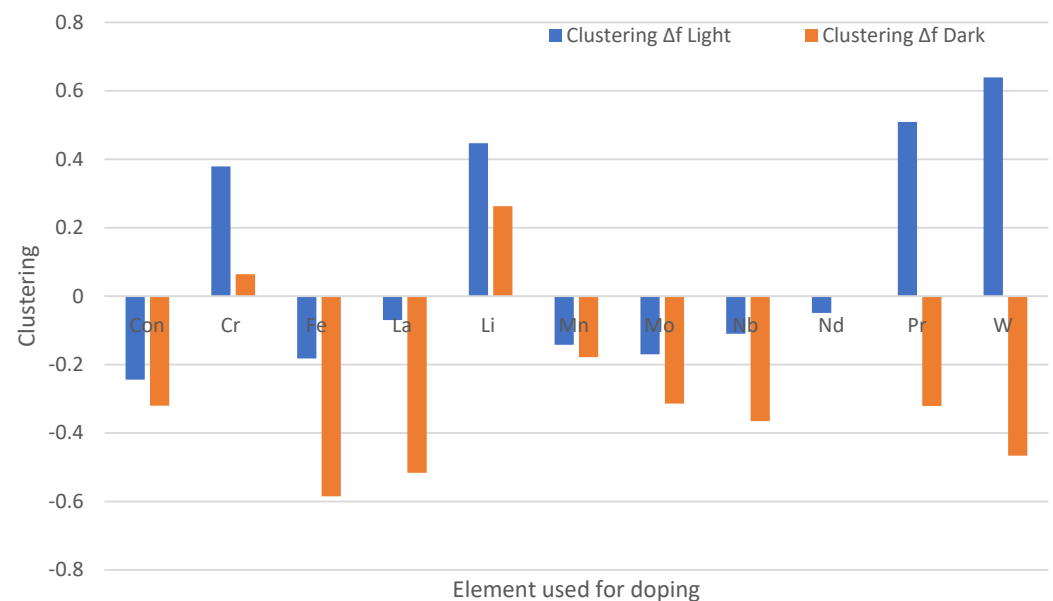


**Figure 8.** Clustering of fungal growth on paint surfaces doped with 0.25% of the elements: Con = control, Cr = chromium, Fe = iron, La = lanthanum, Li = lithium, Mn = manganese, Mo = molybdenum, Nb = niobium, Nd = neodymium, Pr = praseodymium and W = tungsten.

## 4. Discussion

### 4.1. Effect of Paints on Outdoor Colonisation by Fungi

Comparisons were made of a range of paint formulations to withstand fungal colonisation from the outdoor environment. Different paint formulations were placed outside and included TiO<sub>2</sub>. These included acrylic, siloxane and silicone paints. It was found that a wider range of fungal species was observed on the acrylic and siloxane paints than on the silicone paint. This suggests that the chemistry of the paint formulation enabled the growth of more different fungal species over time. In agreement with the results from this work, Cappitelli et al. [22] tested 29 synthetic resins that were used as paint-binding media, including acrylic, alkyd and poly (vinyl acetate) polymers, for their potential susceptibility to fungal degradation, and found that within a few days of inoculation, *Aspergillus niger* was the most copious fungus on the biodegraded resins. Wirth et al. [23] demonstrated that over periods of 4 and 10 weeks, the results showed more severe deterioration of the samples coated with acrylic paint, and at 10 weeks, the worst case reached a grade below. Further, they found *Aspergillus* spp. and *Aureobasidium* fungi were the most dominant species, whereas epoxy paint favoured the growth of *Penicillium* spp. and *Aspergillus* spp. In agreement, our results, which were carried out on different paints, identified mainly *Aspergillus* spp. and *Penicillium* spp. as the main types of colonising fungi, which is perhaps to be expected since they are very common in the environment.

Although some fungal species were persistent throughout this work, there was a change in the total number of species over time. This may be due to the degradation of the paint over time, resulting in a change in available nutrients to support the fungi, although this would need further investigation. If the paint surface were damaged in any way, the resultant change in surface properties might also affect colonisation. In addition, the types of fungi identified also changed over time, which may suggest the replacement of pioneer species with secondary colonisers. At month 3, *Cladsporium* sp. was not recovered from any of the surfaces, and by month 9, *Cladsporium* sp. and yeast 2 were not recovered. Shirakawa et al. [24] reported that *Aureobasidium* was present on the surfaces at the beginning of their tests, but the numbers reduced during the fourth week and recovered in the next weeks, hence suggesting that the presence and concentration of fungi undergo changes as time passes.

### 4.2. Different Paint Formulations in Light and Dark Conditions on Fungal Growth Using UV

Different paint formulations were used to determine whether the growth of fungi was reduced using UV irradiation compared to a reduction in fungal growth under dark conditions. Following UV irradiation, the least growth was demonstrated on the siloxane with a photocatalyst (dark), siloxane with a photocatalyst and biocide (light), acrylic (light or dark), acrylic with a photocatalyst and biocide (dark), and silicate (dark).

The results indicate that the irradiation of the surfaces with UV increased fungal growth for a number of environmental conditions. Fungal UV tolerance is a function of their high melanin content, which can absorb damaging UV photons [25]. It has been shown that *A. niger* spores were highly resistant to high levels of UV-C radiation [26], and previous studies have also reported the presence of melanin in *A. niger* spores as an adaptive trait conferring resistance toward UV-A (315–400) [27]. In addition, exposure to 8 h of natural sunlight for 10 consecutive days was found to increase the UV resistance of *A. niger* spores [28]; thus, it may be that the long-time span of incubation increased their tolerance to UV. It would be interesting to compare the survival of melanin-free spores with the results observed here.

Although a number of surfaces yielded no growth, the addition of biocide to the siloxane and acrylic surfaces under light conditions also increased growth. It may be

suggested that the commercial biocide had an antagonistic effect against the antifungal efficacy of the TiO<sub>2</sub>. The catalyst loading and surrounding matrix is an important factor for an effective photocatalytic process. Acrylic polymers and formulations are proprietary and are used widely as an emulsion resin because they provide coatings with excellent colour retention and have good exterior weathering and durability. Siloxane paints contain straight-chain or cyclic Si-O bonds, often with alkyl groups such as methyl. Silicones are polymeric versions of the siloxane structure. It has also been found that there is an optimal TiO<sub>2</sub> loading [8], whereby the photocatalytic activity rate initially increases with the catalyst loading as the number of active sites increases. However, beyond the optimum loading, certain negative effects come into play [8]. It may be that the addition of the commercial biocide reduced the availability of the TiO<sub>2</sub> to the fungal species, or it may also have acted as a nutrient, thus enabling the additional growth. It is, therefore, important to consider any synergistic characteristics of potential biocide/biocidal combinations in surface modifications.

#### 4.3. Antifungal Efficacy of Doped Paints with Fluorescent Lights

Although titania is itself a good candidate for controlling fungal growth, the paint samples were additionally doped with metals to determine if this would increase the photocatalytic activity of the paint. The metal doping of samples works because the energy of excitation of visible light is too small to directly excite TiO<sub>2</sub>, but it can excite an electron from the valence band across the band gap of the dopant to the conduction band [17]. The hole produced in the valence band stays in the dopant particle, while the electron is transferred to the conduction band of the TiO<sub>2</sub>. The electron transfer from the dopant to the TiO<sub>2</sub> increases the charge separation and efficiency of the photocatalysis process. The separated electron and hole are then free to undergo electron transfer with adsorbates on the surface. Bickley et al. [29] suggested that the recombination lifetime depends on the different preparation methods of the samples that result in crystal structures and surface morphologies with varying defects.

When the paint samples were doped with different elements, the most efficient samples at preventing fungal growth were those surfaces doped with lanthanum, molybdenum or manganese. Although, to the authors' knowledge, there is little or no work on the effect of photocatalytic compounds against lanthanum-based antifungal compounds, such materials have assorted photocatalytic uses [30]. In semiconductors, they can modify the adsorption capabilities of the surface and the complexation of organic pollutants via the lanthanides' f-orbitals, resulting in an improved photocatalytic reaction since they possess an electron configuration of [Xe], i.e., 4f15d16s2 that has incomplete d- and f-orbitals, which reduces electron trapping and constrains their recombination [31]. Molybdenum ions have been found to be aggressive, and the selective capture of photogenerated electrons of Mo<sup>6+</sup> gives Mo<sup>5+</sup>, which produces an increase of holes and, therefore, OH• radicals at the pigment surface [32]. Molybdenum trioxide nanoparticles used with photocatalysis have further demonstrated enhanced antifungal activity against *A. niger* and *Aspergillus fumigatus* [33]. Manganese has shown photocatalytic activity when used as manganese (II) divanadate nano pebbles against *A. niger* [34].

The results also demonstrated that there was low growth of *A. niger* on some samples that were incubated in the dark. Although the lack of light may reduce fungal growth, some metals have shown antimicrobial activities, and so this may have influenced fungal growth. However, the efficacy of the antifungals is very much dependent on the metal complex and concentrations used. For example, metal complexes of La (III) with amino Schiff base ligands, tested against *Aspergillus flavus*, were not found to be antifungal [35]. These differences can be explained by the complexes that such metals are used in and the chemical

availability to which they become available to the fungi. Antifungal activity using coatings of molybdenum trioxide against *Aspergillus fumigatus* has also been demonstrated [36], and metal complexes of tungsten with penicillinate complexes have been shown to have antimicrobial activity against *Aspergillus flavus* [37]. The antifungal activity of  $\text{MnTeO}_3$  [38], iron oxide nanoparticles [39] and tungsten oxide nanocomposites has also further been shown against *A. niger* [40].

The results also found that some of the doped paints increased fungal growth under light conditions. All fungi depend on certain metals for growth and proliferation; however, in the cell, as redox-active metals cycle between two oxidation states, the redox properties can make excess transition elements toxic due to highly reactive oxygen species, which damage lipids, DNA and proteins [41]. In addition, once an organism is exposed to metals, antioxidant defence systems are activated in fungi, and tolerance of *A. niger* to Cd (II) has been shown to be correlated with the heavy metal uptake, reactive oxygen species generation in the cells and the efficiency of an antioxidative defence system [42]. Fungi may have the ability to extract valuable metals such as lithium, allowing the fungi to grow at lower concentrations of the metal, but at higher concentrations, the toxicity of the extracted metals can inhibit fungal growth and result in organic acid production [43]. For example, although the growth of *A. niger* has been shown to be inhibited by chromium (VI) ions, it can also grow in lower levels [44]. In addition, some metals can protect the organisms. Kemp et al. [32] showed that the presence of  $\text{Cr}^{3+}$ -coated  $\text{TiO}_2$  in a sunscreen preparation protected DNA from enhanced degradation. Fungal tolerance can also be demonstrated by some fungal species. Shumilov et al. further showed that *Aspergillus niveoglaucus* demonstrated tolerance to neodymium.

Multifractal analysis (MFA) of the density, dispersion and clustering of the fungal growth across the metal-doped paint surfaces demonstrated that, following incubation in light, more dense fungal colonies were observed, but only for the paint samples containing praseodymium, tungsten and molybdenum, whereas under dark conditions, more dense fungal colonies were demonstrated for chromium, lithium and manganese. Most of the surfaces demonstrated heterogeneous surface coverage by the fungi, but the most heterogeneous dispersion of fungi was demonstrated on the paint samples with an addition of iron, lithium, manganese or molybdenum, whilst the most homogeneous dispersion of the fungi was observed on paint surfaces containing praseodymium. For lithium containing paint surfaces, fungi growth was dispersed across the surface in a symmetrical fashion. The surfaces that were incubated in the dark demonstrated less clustering than those incubated in the light. The most clustering of the fungi was found on the paint samples doped with tungsten, praseodymium, lithium and chromium, whilst the least clustering of the fungi was demonstrated on the surfaces that were doped with iron, lanthanum and tungsten. Work on the binding of *A. niger* conidia to anionic and cationic surfaces demonstrated that surface wettability affected the density and dispersion of fungal conidia, whilst clustering on the surfaces was affected by the spore shape [45]. This suggests that the differences in the surface properties and in the fungal species, if affected by the addition of metal ions, also affected the density, distribution and clustering of the fungal growth on the surfaces; but, further work would be needed to investigate this phenomenon. The use of multifractal analysis to evaluate fungal growth on surfaces provides a novel approach to describe the nature of the surface coverage and merits further investigation.

## 5. Conclusions

Following work on the resistance of paint surfaces to colonisation by fungi, it was demonstrated that the composition of the paint influenced the amount of growth (coverage) and range of species (number) of fungi. The growth, following UV irradiation, was



influenced by the composition of the paint and the addition of biocide. This was important since the addition of biocide increased fungal growth in certain conditions. Doping of the paints with different elements, in some cases, increased the antifungal effect of the paints and indicated that consideration of the impact of combinations of biocides should be made prior to implementation. Multifractal analysis revealed that the light exposure and paint composition affected the density of the fungal growth across the surfaces, although most of the surfaces demonstrated heterogeneous surface coverage. The clustering of the fungal colonies was influenced by whether it was grown in light or dark conditions. Thus, this work demonstrates the multifactorial influences that result in the fungal colonisation of paint surfaces. Since the addition of biocides and dopants affects the type, species and amount of fungal growth, a single solution for the prevention of all fungal colonisations on all different types of paints may not be possible; complete prevention of fungal growth is unlikely, and thus, a more controlled/targeted approach might be more useful. Thus, a much deeper understanding of how fungi colonise and can be controlled on painted surfaces is required because using the incorrect combinations of biocidal approaches may result in increased fungal colonisation.

**Author Contributions:** Writing—review & editing, K.A.W., M.B., J.V., C.H., N.S.A., S.L., M.E. and L.C.; Writing—original draft, K.A.W.; Methodology, K.A.W., M.B., S.L., M.E., N.S.A. and C.H.; Investigation, M.B. and S.L.; Formal analysis, K.A.W., M.B. and S.L.; Visualization, J.V., C.H. and N.S.A.; Validation, J.V., C.H. and N.S.A.; Supervision, J.V., M.E., C.H. and N.S.A.; Resources, J.V., M.E., N.S.A. and S.L.; Project administration, N.S.A.; Funding acquisition, C.H. and N.S.A.; Conceptualization, C.H., J.V. and N.S.A.; Data curation, K.A.W., M.B., J.V., C.H., N.S.A. and S.L. All authors have read and agreed to the published version of the manuscript.

**Funding:** The authors would like to thank Tronox PLC (Formerly Crystal Global) for providing the funding for this work.

**Institutional Review Board Statement:** Not applicable.

**Informed Consent Statement:** Not applicable.

**Data Availability Statement:** Original/source data for the figures and data in the paper are available from the lead contact upon reasonable request.

**Conflicts of Interest:** The authors declare that this study was funded by Tronox PLC (Formerly Crystal Global).

## References

1. Allen, N.S.; Edge, M.; Verran, J.; Stratton, J.; Maltby, J.; Bygott, C. Photocatalytic titania based surfaces: Environmental benefits. *Polym. Degrad. Stab.* **2008**, *93*, 1632–1646. [[CrossRef](#)]
2. Fujishima, A.; Rao, T.N.; Tryk, D.A. Titanium dioxide photocatalysis. *J. Photochem. Photobiol. C Photochem. Rev.* **2000**, *1*, 1–21. [[CrossRef](#)]
3. Buxbaum, G.; Pfaff, G. (Eds.) *Industrial Inorganic Pigments*, 3rd ed.; WILEY-VCH Verlag GmbH&Co: Hoboken, NJ, USA, 2005.
4. Wakamura, M. Antibacterial, Antifouling Paint for Construction Materials and Construction Materials Coated Therewith. U.S. Patent US7157503B2, 2 January 2007.
5. Goodwin, G.; Stratton, J.; McIntyre, R. Coating Composition Having Surface Depolluting Properties. U.S. Patent US20070167551A1, 3 July 2007.
6. Gambogi, J. Titanium and Titanium Dioxide. In *Mineral Commodity Summaries*; U.S. Department of the Interior, U.S. Geological Survey, Science for a Changing World: Reston, VA, USA, 2009; pp. 176–177.
7. Stratton, J. Depolluting Coating Composition. U.S. Patent US20080097018A1, 24 April 2008.
8. Caballero, L.; Whitehead, K.A.; Allen, N.S.; Verran, J. Inactivation of *E. coli* on immobilized TiO<sub>2</sub> using fluorescent light. *J. Photochem. Photobiol. A: Chem.* **2009**, *202*, 92–98. [[CrossRef](#)]
9. Caballero, L.; Whitehead, K.A.; Allen, N.S.; Verran, J. Photoinactivation of *Escherichia coli* on acrylic paint formulations using fluorescent light. *Dye. Pigment.* **2010**, *86*, 56–62. [[CrossRef](#)]

10. Caballero, L.; Whitehead, K.A.; Allen, N.A.; Verran, J. Photocatalytic inactivation of *Escherichia coli* using doped titanium dioxide under fluorescent irradiation. *J. Photochem. Photobiol. A Chem.* **2014**, *276*, 50–57. [[CrossRef](#)]
11. Chatterjee, D.; Dasgupta, S. Visible light induced photocatalytic degradation of organic pollutants. *J. Photochem. Photobiol. C: Photochem. Rev.* **2005**, *6*, 186–205. [[CrossRef](#)]
12. Chen, J.; Poon, C. Photocatalytic construction and building materials: From fundamentals to applications. *Build. Environ.* **2009**, *44*, 1899–1906. [[CrossRef](#)]
13. Benabbou, A.K.; Derriche, Z.; Felix, C.; Lejeune, P.; Guillard, C. Photocatalytic inactivation of *Escherichia coli*: Effect of concentration of TiO<sub>2</sub> and microorganism, nature, and intensity of UV irradiation. *Appl. Cat. B Environ.* **2007**, *76*, 257–263. [[CrossRef](#)]
14. Pichat, P.; Guillard, C.; Amalric, L.; Renard, A.; Plaidy, O. Assessment of the importance of the role of H<sub>2</sub>O<sub>2</sub> and O<sub>2</sub><sup>•-</sup> in the photocatalytic degradation of 1, 2-dimethoxybenzene. *Solar Energy Mat. Solar Cells.* **1995**, *38*, 391–399. [[CrossRef](#)]
15. Rincon, A.G.; Pulgarin, C. Photocatalytical inactivation of *E. coli*: Effect of (continuous-intermittent) light intensity and of (suspended-fixed) TiO<sub>2</sub> concentration. *Appl. Cat. B Environ.* **2003**, *44*, 263–284. [[CrossRef](#)]
16. ASTM D5590-17; Standard Test Method for Determining the Resistance of Paint Films and Related Coatings to Fungal Defacement by Accelerated Four-Week Agar Plate Assay. ASTM International D5590 Standard Test Method for Determining the Resistance of Paint Films and Related Coatings to Fungal Defacement by Accelerated Four-Week Agar Plate Assay. ASTM: West Conshohocken, PA, USA, 2021.
17. Linsebigler, A.L.; Lu, G.Q.; Yates, J.T. Photocatalysis on TiO<sub>2</sub> surfaces—principles, mechanisms, and selected results. *Chem. Rev.* **1995**, *95*, 735–758. [[CrossRef](#)]
18. Solomon, D.H.; Hawthorne, D.G. *Chemistry of Pigments and Fillers*; Wiley: Hoboken, NJ, USA, 1983; pp. 51–80.
19. Koleske, J.V. (Ed.) *Paint and Coating Testing Manual*, 14th ed. ASTM International: West Conshohocken, PA, USA, 1995.
20. Lynch, S. *Python for Scientific Computing and Artificial Intelligence*; CRC Press: Boca Raton, FL, USA, 2023.
21. Lynch, S. *Dynamical Systems with Applications Using MATLAB*, 3rd ed.; Springer International Publishing: New York, NY, USA, 2024; *in press*.
22. Cappitelli, F.; Vicini, S.; Piaggio, P.; Abbruscato, P.; Princi, E.; Casadevall, A.; Nosanchuk, J.D.; Zanardini, E. Investigation of Fungal Deterioration of Synthetic Paint Binders Using Vibrational Spectroscopic Techniques. *Macromol. Biosci.* **2005**, *5*, 49–57. [[CrossRef](#)] [[PubMed](#)]
23. Wirth, A.; Pacheco, F.; Toma, N.; Valiati, V.; Tutikian, V.; Gomes, L. Analysis of fungal growth on different coatings applied to lightweight systems. *Rev. Ing. Construcción* **2019**, *34*, 5–14. [[CrossRef](#)]
24. Shirakawa, M.A.; Gaylarde, C.C.; Gaylarde, P.M.; John, V.; Gambale, W. Fungal Colonization and succession on newly painted buildings and the effect of biocide. *FEMS Microbiol. Ecol.* **2002**, *39*, 165–173. [[CrossRef](#)]
25. Cockell, C.S.; Knowland, J. Ultraviolet radiation screening compounds. *Biol. Rev.* **1999**, *74*, 311–345. [[CrossRef](#)]
26. Cortesão, M.; de Haas, A.; Unterbusch, R.; Fujimori, A.; Schütze, T.; Meyer, V.; Moeller, R. *Aspergillus niger* Spores Are Highly Resistant to Space Radiation. *Front Microbiol.* **2020**, *3*, 560. [[CrossRef](#)]
27. Singaravelan, N.; Grishkan, I.; Beharav, A.; Wakamatsu, K.; Ito, S.; Nevo, E. Adaptive melanin response of the soil fungus *Aspergillus niger* to UV radiation stress at “evolution canyon”, mount carmel, Israel. *PLoS ONE* **2008**, *3*, e2993. [[CrossRef](#)]
28. Taylor-Edmonds, L.; Lichi, T.; Rotstein-Mayer, A.; Mamane, H. The impact of dose, irradiance and growth conditions on *Aspergillus niger* (renamed *A. brasiliensis*) spores low-pressure (LP) UV inactivation. *J. Environ. Sci. Health Part A* **2015**, *50*, 341–347. [[CrossRef](#)]
29. Bickley, R.I.; Gonzalez-Carreno, T.; Lees, J.S.; Palmisano, L.; Tilley, R.J.D. Structural investigation of titanium dioxide photocatalysts. *J. Solid State Chem.* **1991**, *92*, 178–190. [[CrossRef](#)]
30. Jing, L.; Xu, Y.; Liu, J.; Zhou, M.; Xu, H.; Xie, M.; Li, H.; Xie, J. Direct Z-scheme red carbon nitride/rod-like lanthanum vanadate composites with enhanced photodegradation of antibiotic contaminants. *Appl. Cat. B Environ.* **2020**, *277*, 119245. [[CrossRef](#)]
31. Khan, A.A.; Partho, A.T.; Arnab, M.H.; Khyam, M.A.; Kumar, N.; Tahir, M. Recent advances in Lanthanum-based photocatalysts with engineering aspects for photocatalytic hydrogen production: A critical review. *Mat. Sci. Semicond. Process.* **2024**, *184*, 108809. [[CrossRef](#)]
32. Kemp, T.J.; McIntyre, R.A. Photodegradation of DNA induced by modified forms of titanium dioxide. *Prog. React. Kinet. Mech.* **2007**, *32*, 219–229. [[CrossRef](#)]
33. Mir, S.M.; Shaikh, K.R.; Pawar, A.R.; Undre, P.B. Microwave-assisted synthesis and functionalization of nanocrystalline molybdenum trioxide for enhanced antimicrobial and photocatalytic activity. *J. Indian Chem. Soc.* **2024**, *101*, 101288. [[CrossRef](#)]
34. Mallikarjunaswamy, C.; Pramila, S.; Nagaraju, G.; Lakshmi Ranganatha, V. Enhanced photocatalytic, electrochemical and antimicrobial activities of alpha-Mn<sub>2</sub>V<sub>2</sub>O<sub>7</sub> nanopebbles. *J. Mat. Sci. Mat. Elec.* **2021**, *33*, 617–634. Available online: <https://api.semanticscholar.org/CorpusID:244532565> (accessed on 6 September 2024). [[CrossRef](#)]
35. Alghool, S.; Abd El-Halim, H.F.; Abd El-sadek, M.A.; Yahia, I.S.; Wahab, L.A. Synthesis, thermal characterization, and antimicrobial activity of lanthanum, cerium, and thorium complexes of amino acid Schiff base ligand. *J. Thermal Anal. Calorim.* **2013**, *112*, 671. [[CrossRef](#)]

36. Tétault, N.; Gbaguidi-Haore, H.; Bertrand, X.; Quentin, R.; van der Mee-Marquet, N. Biocidal activity of metalloacid-coated surfaces against multidrug-resistant microorganisms. *Antimicrob. Resist. Infect. Control.* **2012**, *14*, 35. [[CrossRef](#)] [[PubMed](#)]
37. El-Habeeb, A.A.; Refat, M.S. Synthesis and Spectroscopic Investigations of Four New Y(III), Ge(IV), W(VI) and Si(IV) Penicillin Antibiotic Drug Complexes. *Spectrosc. Spectr. Anal.* **2019**, *39*, 2982–2988.
38. Umar, M.; Ajaz, H.; Javed, M.; Mansoor, S.; Iqbal, S.; Rauf, A.; Alhujaily, A.; Awwad, N.S.; Ibrahim, H.S.; Althobiti, R.A.; et al. Design of a highly efficient heterostructure of transition metal tellurides with outstanding photocatalytic and antimicrobial potential. *J. Saudi Chem. Soc.* **2023**, *27*, 101760. [[CrossRef](#)]
39. Mohandoss, N.; Renganathan, S.; Subramaniyan, V.; Nagarajan, P.; Elavarasan, V.; Subramaniyan, P.; Vijayakumar, S. Investigation of Biofabricated Iron Oxide Nanoparticles for Antimicrobial and Anticancer Efficiencies. *Appl. Sci.* **2022**, *12*, 12986. [[CrossRef](#)]
40. Ismail, A.S.; Tawfik, S.M.; Mady, A.H.; Lee, Y.-I. Preparation, Properties, and Microbial Impact of Tungsten (VI) Oxide and Zinc (II) Oxide Nanoparticles Enriched Polyethylene Sebacate Nanocomposites. *Polymers* **2021**, *13*, 718. [[CrossRef](#)]
41. Blatzer, M.; Latgé, J.P. Metal-homeostasis in the pathobiology of the opportunistic human fungal pathogen *Aspergillus fumigatus*. *Curr. Opin. Microbiol.* **2017**, *40*, 152–159. [[CrossRef](#)] [[PubMed](#)]
42. Todorova, D.; Nedeva, D.; Abrashev, R.; Tsekova, K. Cd (II) stress response during the growth of *Aspergillus niger* B 77. *J. Appl. Microbiol.* **2008**, *104*, 178–184. [[CrossRef](#)] [[PubMed](#)]
43. Lobos, A.; Harwood, V.J.; Scott, K.M.; Cunningham, J.A. Tolerance of three fungal species to lithium and cobalt: Implications for bioleaching of spent rechargeable Li-ion batteries. *J. Appl. Microbiol.* **2021**, *131*, 743–755. [[CrossRef](#)]
44. Dursun, A.Y.; Uslu, G.; Cuci, Y.; Aksu, Z. Bioaccumulation of copper(II), lead(II) and chromium(VI) by growing *Aspergillus niger*. *Process Biochem.* **2003**, *38*, 1647–1651. [[CrossRef](#)]
45. Whitehead, K.A.; Lynch, S.; Amin, M.; Deisenroth, T.; Liauw, C.M.; Verran, J. Effects of Cationic and Anionic Surfaces on the Perpendicular and Lateral Forces and Binding of *Aspergillus niger* Conidia. *Nanomaterials* **2023**, *11*, 2932. [[CrossRef](#)] [[PubMed](#)]

**Disclaimer/Publisher's Note:** The statements, opinions and data contained in all publications are solely those of the individual author(s) and contributor(s) and not of MDPI and/or the editor(s). MDPI and/or the editor(s) disclaim responsibility for any injury to people or property resulting from any ideas, methods, instructions or products referred to in the content.